Eur. J. Mineral.
2017, **29**, 499–510

Copper oxosulphates from fumaroles of Tolbachik volcano: puninite, $Na_2Cu_3O(SO_4)_3$ – a new mineral species and structure refinements of kamchatkite and alumoklyuchevskite

Oleg I. SIIDRA[1,*], Evgenii V. NAZARCHUK[1], Anatoly N. ZAITSEV[2], Evgeniya A. LUKINA[1],
Evgeniya Y. AVDONTSEVA[1], Lidiya P. VERGASOVA[3], Natalia S. VLASENKO[4], Stanislav K. FILATOV[1],
Rick TURNER[5] and Gennady A. KARPOV[3]

[1] Department of Crystallography, St. Petersburg State University, University emb. 7/9, 199034 St. Petersburg, Russia
*Corresponding author, e-mail: o.siidra@spbu.ru
[2] Department of Mineralogy, St. Petersburg State University, University emb. 7/9, 199034 St. Petersburg, Russia
[3] Institute of Volcanology and Seismology, Russian Academy of Sciences, Bulvar Piypa 9,
683006 Petropavlovsk-Kamchatskiy, Russia
[4] Research Park, Resource Centre Geomodel, St. Petersburg State University, University emb. 7/9, 199034 St. Petersburg, Russia
[5] The Drey, Allington Track, Allington, Salisbury SP4 0DD, Wiltshire, UK

Abstract: Typical characteristics of many anhydrous sulphates of exhalative origin at fumaroles at the Second scoria cone of the Northern Breakthrough of the Great Tolbachik Fissure Eruption, Tolbachik volcano, Kamchatka, Russia, are the presence of additional oxygen atoms (O_a) in the composition. Recent field works on the fumaroles of the Second scoria cone in 2014 and 2015 resulted in discovery of a new mineral species, puninite, and collection of fresh alumoklyuchevskite and kamchatkite samples which allowed the re-refinement of crystal structures. The crystal structure of kamchatkite, $KCu_3O(SO_4)_2Cl$, was solved and refined in *Pnma* space group ($a = 9.755(2)$, $b = 7.0152(15)$, $c = 12.886(3)$ Å, $V = 881.8(3)$ Å^3, $R_1 = 0.021$), whereas alumoklyuchevskite, $K_3Cu_3AlO_2(SO_4)_4$, is triclinic, $P\overline{1}$ ($a = 4.952(3)$, $b = 11.978(6)$, $c = 14.626(12)$ Å, $\alpha = 87.119(9)$, $\beta = 80.251(9)$, $\gamma = 78.070(9)°$, $V = 836.3(9)$ Å^3, $R_1 = 0.049$) in contrast to previously reported data.

The new mineral puninite, ideally $Na_2Cu_3O(SO_4)_3$, was found in sublimates of *Glavnaya Tenoritovaya* fumarole. The mineral is named in honor of the Russian crystallographer Yurii Olegovich Punin (1941–2014). Puninite is closely associated with lammerite-β, tenorite, hematite and anhydrite. Puninite is emerald-green in colour. It is biaxial, optically positive, $\alpha = 1.587(2)$, $\beta = 1.611(2)$, $\gamma = 1.649(2)$, $2V_{calc} = 60°$. The mineral is soluble in water. The empirical formula of puninite based on 13 O atoms is $(Na_{1.76}K_{0.08})_{\Sigma 1.84}(Cu_{2.97}Zn_{0.04})_{\Sigma 3.01}(SO_4)_{3.02}O_{0.92}$. Puninite is the first Na-dominant copper oxosulfate mineral observed on Second scoria cone. It is monoclinic, *C*2/*c*, $a = 17.41(1)$, $b = 9.39(1)$, $c = 14.40(1)$ Å, $\beta = 112.04(7)°$, $V = 2183(2)$ Å^3, $Z = 8$. The eight strongest lines of the X-ray powder diffraction pattern are (*I-d-hkl*): 100-8.058-200, 18.88-6.675- $00\overline{2}$, 28.47-6.466- $20\overline{2}$, 14.1-4.398-202, 17.37-4.247- $11\overline{3}$, 33.89-3.839- $02\overline{2}$, 29.15-2.854- $22\overline{4}$, 14.95-2.724- $02\overline{4}$. Puninite is structurally related to euchlorine, $NaKCu_3O(SO_4)_3$ and to fedotovite, $K_2Cu_3O(SO_4)_3$. The unit-cell *a* parameter value is very sensitive to the K-Na ratio in “euchlorine group” minerals. The crystal structure of puninite ($R_1 = 0.035$) is based on oxocentred $[O_2Cu_6]^{8+}$ dimers. Four sulphate tetrahedra are ‘face-to-face’ attached to the dimers, whereas the other sulphate tetrahedral groups provide their linkage in two dimensions. The structural architecture of all the copper-oxosulphate exhalative minerals described in this paper can be described as being organized via a “*host–guest*” principle.

Key-words: puninite; new mineral; kamchatkite; alumoklyuchevskite; sulphates; oxocentred tetrahedra; volcanic exhalations; crystal structure; host–guest structures; Second scoria cone; Tolbachik.

1. Introduction

Fumarolic activity taking place after the Great Tolbachik Fissure eruption (GTFE) that occurred in 1975–1976 in Kamchatka peninsula, Russia (Fedotov and Markhinin, 1983; Vergasova and Filatov, 2012) is characterized by the great variety of sulphate minerals. Most of these minerals are anhydrous, in contrast to the majority of known sulphate minerals which contain additional water molecules or hydroxyl groups (Alpers *et al.*, 2000). To date, more than 20 sulphate mineral species have been discovered in fumaroles of the Second scoria cone,

0935-1221/17/0029-2619 $ 5.40
DOI: 10.1127/ejm/2017/0029-2619

Northern Breakthrough, GTFE. Typical characteristics of many anhydrous sulphates of exhalative origin at this locality are the presence of additional oxygen atoms (O_a) in the composition: for example, piypite, $K_4Cu_4O_2(SO_4)_4{\cdot}(Na,Cu)Cl$ (Filatov & Vergasova, 1989); fedotovite, $K_2Cu_3O(SO_4)_3$, euchlorine, $KNaCu_3O(SO_4)_3$ (Vergasova *et al.*, 1988a); kamchatkite, $KCu_3OCl(SO_4)_2$ (Vergasova *et al.*, 1988b); klyuchevskite, $K_3Cu_3Fe^{3+}O_2(SO_4)_4$ (Vergasova *et al.*, 1989); alumoklyuchevskite, $K_3Cu_3AlO_2(SO_4)_4$ (Gorskaya *et al.*, 1995); dolerophanite, $Cu_2O(SO_4)$ (Effenberger, 1985); nabokoite, $Cu_7TeO_4(SO_4)_5{\cdot}KCl$ (Popova *et al.*, 1987); atlasovite, $Cu_6Fe^{3+}Bi^{3+}O_4(SO_4)_5{\cdot}KCl$ (Popova *et al.*, 1987); vergasovaite, $Cu_3O[(Mo,S)O_4)](SO_4)$ (Bykova *et al.*, 1998); wulffite, $K_3NaCu_4O_2(SO_4)_4$, and parawulffite, $K_5Na_3Cu_8O_4(SO_4)_8$ (Pekov *et al.*, 2014); cryptochalcite, $K_2Cu_5O(SO_4)_5$ (Pekov *et al.*, 2015c), which all contain O atoms that do not participate in strongly bonded $(SO_4)^{2-}$ complexes. Volcanic gases of the GTFE are enriched in copper (Meniaylov *et al.*, 1980) and many of the sulphate minerals contain this metal as essential component, with consequent formation of unique mineral assemblages. The O_a atoms in the structures of such sulphate minerals are tetrahedrally coordinated by Cu, with formation of oxocentered OCu_4 tetrahedra (Krivovichev *et al.*, 2013) polymerized into a variety of structural units with different dimensionality. Note also that all of the copper oxosulphate minerals listed above (except vergasovaite) contain alkali elements (K and/or Na). Potassium dominates in the composition of these minerals, whereas Na is an essential component in euchlorine, wulffite and parawulffite only. Euchlorine is one of the most abundant minerals in fumaroles of the Second scoria cone (GTFE) and Naboko scoria cone, Tolbachik Fissure eruption in 2012–2013 (TFE) (Volynets *et al.*, 2013). The presence of the oxocentered OCu_4 tetrahedra in the structures of exhalative minerals from fumaroles of the Second scoria cone suggested a mechanism of metal (mainly copper) transport by volcanic gases in the form of similar tetrahedral complexes (Filatov *et al.*, 1992).

Kamchatkite, $KCu_3O(SO_4)_2Cl$ (Vergasova *et al.*, 1988b) was discovered in the exhalative sulphate assemblages of the Yadovitaya (Poisonous) Fumarole. The crystal structure of kamchatkite was refined in the non-centrosymmetric $Pna2_1$ space group to $R_1 = 0.055$ (Varaksina *et al.*, 1990). Alumoklyuchevskite, $K_3Cu_3AlO_2(SO_4)_4$ is isotypic to klyuchevskite, $K_3Cu_3Fe^{3+}O_2(SO_4)_4$ (Vergasova *et al.*, 1989) and was discovered in 1995 (Gorskaya *et al.*, 1995) in the samples collected earlier, soon after eruption in 1976–1977; however, the only structural information available to date for both minerals is of rather poor quality ($R_1 = 13\%$: Krivovichev *et al.*, 2009). Kamchatkite and alumoklyuchevskite are unstable in open air at ambient conditions and hydrate with subsequent decomposition as do all the other copper oxosulphates of exhalative origin. Recent field works on the fumaroles of the Second scoria cone in 2014 and 2015 resulted in collection of fresh alumoklyuchevskite and kamchatkite samples which allowed the re-refinement of crystal structures, reported here.

The new mineral puninite, $Na_2Cu_3O(SO_4)_3$, was also discovered in fresh samples collected by O.I.S. and E.A.L. in the *Glavnaya Tenoritovaya* fumarole in 2014. Puninite (Cyrillic: пунинит) is named in honour of Professor Yurii Olegovich Punin (Юрий Олегович Пунин) (1941–2014), who worked for 45 years at Department of Crystallography, St. Petersburg State University, Russia. Yurii Punin was an outstanding scientist in the field of Crystallography and Crystal Growth. The mineral and mineral name have been approved by the Commission on New Minerals and Mineral Names of the International Mineralogical Association (2015-012). Type material is deposited in the collections of the Mineralogical Museum, Department of Mineralogy, St Petersburg State University, St Petersburg, Russia, catalogue number 19638.

2. Locality and occurrence

Puninite, kamchatkite and alumoklyuchevskite were found in the *Glavnaya Tenoritovaya* fumarole (Pekov *et al.*, 2015a) on the Second scoria cone of the Northern Breakthrough of the GTFE on Kamchatka peninsula, Russia. The Second scoria cone is located 18 km SSW of the active volcano Ploskiy Tolbachik. The temperature of gases in the sampling location was about 320 °C. Puninite occurs as crystalline crusts (Fig. 1), individual crystals up to 10 × 30 × 50 μm (usually from 5 to 20 μm in size) and irregularly shaped grains. Puninite is closely associated with lammerite-β, tenorite, hematite and anhydrite. The kamchatkite and alumokluchevskite used in this study have the same macroscopic appearance as those described by Vergasova *et al.* (1988b) and Gorskaya *et al.* (1995). Kamchatkite occurs in association with chalcocyanite, coparsite, and unidentified Cs-Cu-Cl selenite and Cu-Cl arsenate (Fig. 2).

3. Experimental procedure

3.1. Physical and optical properties of puninite

Puninite is emerald-green in colour, has a greenish streak and vitreous lustre. The mineral is brittle with uneven fracture and perfect cleavage on {100}. Hardness corresponds to 2–3 on the Mohs' scale. The density could not be measured due to sample paucity, but it has been calculated as 3.284 g cm^{-3} using structural data and the empirical formula. No fluorescence is detected. Under the microscope, puninite is pale green with very weak pleochroism. It is biaxial, optically positive, $\alpha = 1.562(2)$, $\beta = 1.591(2)$, $\gamma = 1.634(2)$ (589 nm), $2V$ (meas.) moderately large, $2V_{calc} = 80.7°$. The mineral is soluble in water. Compatibility, $1 - (K_p/K_c) = -0.035$, is excellent (Mandarino, 1981).

3.2. Chemical composition

Three crystals (40 × 40 to 40 × 20 μm) of puninite were mounted in epoxy resin and polished with oil suspension. The mineral was analysed using a Hitachi S-3400N

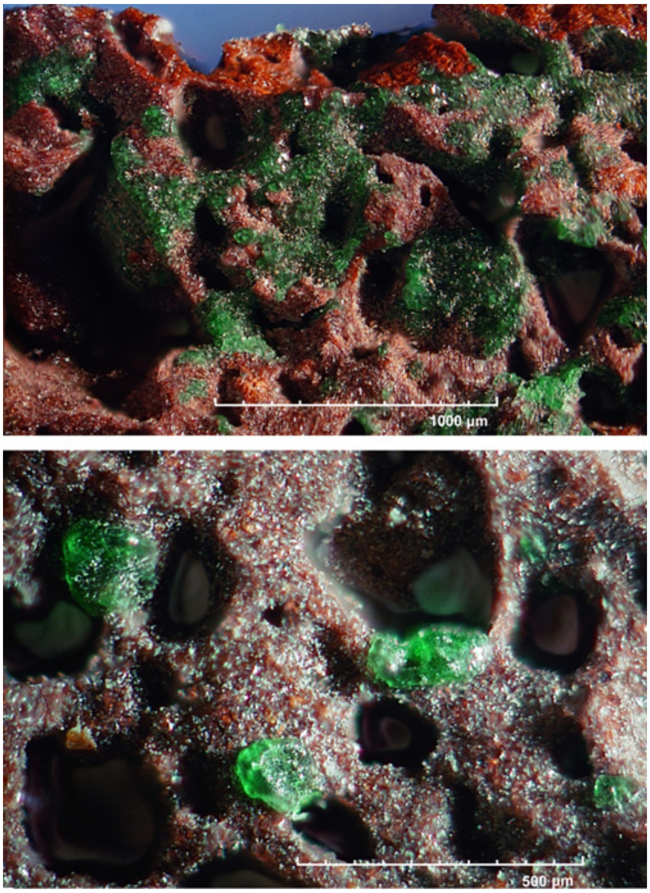

Fig. 1. Puninite green crystalline aggregates (above) and enlarged puninite individual crystals (below). (Online version in colour.)

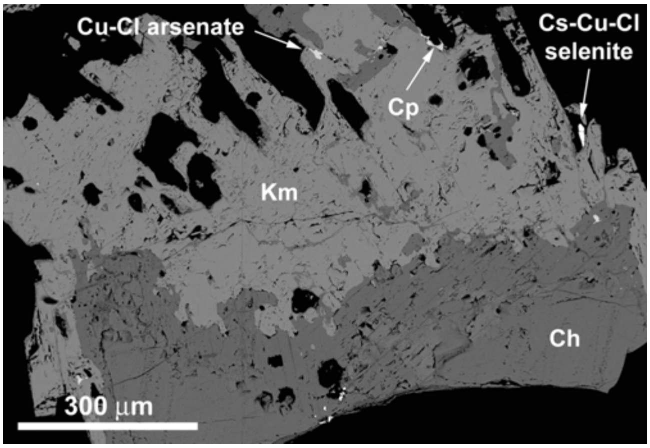

Fig. 2. Back-scattered electron microscope image of kamchatkite (Km) associated with chalcocyanite (Ch). Some other minerals include: coparsite (Cp), an unidentified Cu arsenate-chloride and an unidentified Cs-Cu selenite chloride, $Cs_2Cu_{8.5}O_{2.5}(SeO_3)_3Cl_{10}$.

scanning electron microscope equipped with an Oxford Instruments INCA energy-dispersive spectrometer (SEM/EDS). The electron beam accelerating voltage was 20 kV, and beam current 2.5 nA as measured by a Faraday cup. The X-ray acquisition live-time was 30 s, and X-ray processing time '5' for analysis. The mineral is unstable under a spot electron beam, with strong sodium loss during analysis; therefore, a defocused beam (3–4 μm) was used for the analyses. Wider beam diameter could not be used due to the presence of thick cracks on the mineral surface. X-ray matrix correction was carried out automatically by the Oxford Instruments INCA version of the Pouchou and Pichoir (XPP) routine. Well characterised synthetic compounds and minerals were used for standardisation. System (gain) calibration was performed on Co.

The results of ten analyses are summarized in Table 1. In addition to major elements Na, Cu and S the mineral contains minor K and Zn. No other elements with $Z \geq 9$ were found during the SEM/EDS study. Detection of the low amount Zn in puninite is problematic due to partial overlap of elemental X-ray peaks of Zn $L\alpha$ (1.012 keV) with Cu $L\alpha$ (0.930 keV) and Na $K\alpha$ (1.041 keV) on EDS spectra. Application of wavelength-dispersive spectroscopy (WDS), TAP crystal, 10 nA beam current, scan speed 0.25 Å per minute, confirmed the presence of the Zn peak, but the element could not be quantitatively analysed due to rapid and strong surface damage during scanning. The empirical formula of puninite based on 13 O atoms is $(Na_{1.76}K_{0.08})_{\Sigma 1.84}(Cu_{2.97}Zn_{0.04})_{\Sigma 3.01}(SO_4)_{3.02}O_{0.92}$ and the simplified mineral formula is $Na_2Cu_3O(SO_4)_3$, corresponding to (in wt.%) $Na_2O = 11.46$, $CuO = 44.13$ and $SO_3 = 44.41$.

Alumoklyuchevskite and kamchatkite were analysed using the same instrument, but with slightly different analytical conditions: an electron beam current of 1.0 nA and beam diameter up to 10 μm.

Alumoklyuchevskite forms a solid solution with klyuchevskite, with an Al_2O_3 content between 6.9 and 1.0 wt.% and Fe_2O_3 content between 1.3 and 9.2 wt.% (Gorskaya *et al.*, 1995). The studied sample contains 4.9 wt.% Al_2O_3 and 2.7 wt.% Fe_2O_3 which corresponds to 73.4 mol.% $K_3Cu_3Al(SO_4)_4O_2$ and 26.6 mol.% $K_3Cu_3Fe^{3+}(SO_4)_4O_2$ end-members (Table 1). The composition of kamchatkite (Table 1) is close to the ideal formula $KCu_3(SO_4)_2OCl$, with up to 0.5 wt.% ZnO.

3.3. X-ray crystallography

Powder X-ray diffraction data for puninite were obtained using a Rigaku R-AXIS Rapid II single-crystal diffractometer equipped with cylindrical image plate detector, in Debye-Scherrer geometry (with $d = 127.4$ mm), after crushing the crystals fragments used for the single-crystal analysis. Data (in Å for Co$K\alpha$) are given in Table 2. The unit-cell parameters were refined in the monoclinic unit cell, space group $C2/c$, $a = 17.41(1)$, $b = 9.39(1)$, $c = 14.40(1)$ Å, $\beta = 112.04(7)°$, $V = 2183(2)$ Å^3, $Z = 8$.

Single-crystal X-ray analysis of puninite, kamchatkite and alumoklyuchevskite was carried out using a Bruker SMART diffractometer equipped with an APEX II CCD detector operating with Mo$K\alpha$ radiation at 50 kV and 40 mA. A single green translucent block-shaped puninite crystal with dimensions of 0.16 × 0.12 × 0.14 mm, a green prismatic kamchatkite crystal of 0.15 × 0.10 × 0.10 mm and a dark-green, acicular alumoklyuchevskite crystal of

Table 1. Compositional data for puninite, kamchatkite and alumoklyuchevskite, wt.%.

Mineral	Puninite			Kamchatkite			Alumoklyuchevskite		
	Average (10)	Min	Max	Average (13)	Min	Max	Average (5)	Min	Max
Na_2O	9.98	8.04	10.85						
K_2O	0.63	0.55	0.71	9.64	9.41	9.95	18.18	17.99	18.44
Rb_2O							0.54	0.48	0.61
CuO	43.21	42.50	44.57	50.61	49.19	51.93	31.47	30.72	32.06
ZnO	0.66	0.56	0.81	0.35	0.22	0.49			
Al_2O_3							4.90	4.72	5.06
Fe_2O_3							2.73	2.38	3.03
SO_3	44.33	43.03	44.85	34.34	33.73	35.19	42.44	42.29	42.70
Cl				7.44	7.23	7.58			
$–O{=}Cl_2$				1.68					
Total	98.81			100.70			100.26		
Atoms per formula unit calculated for									
	O = 13			O = 10			O = 18		
Na	1.76								
K	0.07			0.96			2.92		
Rb							0.04		
Cu	2.97			2.98			3.00		
Zn	0.04			0.02					
Al							0.73		
Fe							0.26		
S	3.02			2.01			4.01		
Cl				0.98					

0.20 × 0.06 × 0.07 mm were chosen for X-ray diffraction study. More than a hemisphere of data was collected with a frame width of 0.5° in ω, and 10 s counting time for each frame for all of the described minerals. The data were integrated and corrected for absorption using a multiscan type model using the Bruker programs APEX and SADABS. Puninite is monoclinic, space group *C*2/*c*, $a = 17.3885(13)$, $b = 9.4009(8)$, $c = 14.4045(11)$ Å, $\beta = 112.039(2)°$, $V = 2182.6(3)$ Å^3, $Z = 8$ (Table 3). The atom coordinates for euchlorine published by Scordari & Stasi (1990) were used initially and the structure was successfully refined with the use of SHELX software package (Sheldrick, 2015). Atom coordinates, bond-valence sums and thermal displacement parameters for puninite are given in Table 4 and selected interatomic distances in Table 5.

The unit-cell parameters obtained for kamchatkite (Table 3) are very similar to those reported earlier in Varaksina *et al.* (1990). Statistics of diffraction intensities and systematic extinctions for kamchatkite were consistent with the space group *Pnma*. The $|E^2 - 1|$ parameter was equal to 0.915, which clearly indicated a high probability of a centrosymmetric space group (Marsh, 1995) which we confirmed by subsequent structure solution and refinement in *Pnma* ($R_1 = 0.021$) instead of $Pna2_1$ ($R_1 = 0.055$). Comparison of experimental (Vergasova *et al.*, 1988b) and calculated powder patterns for the structural data obtained in this work and after Varaksina *et al.* (1990) are presented in Table S1 freely available as Supplementary Material attached to this article on the GSW website of the journal: http://eurjmin.geoscienceworld.org/. The calculated pattern for kamchatkite is in somewhat better agreement with the observed pattern reported in Vergasova *et al.* (1988b) than the calculated powder pattern for the crystal structure reported in Varaksina *et al.* (1990). Observed discrepancies are due to different space groups.

Alumoklyuchevskite structural data are presented in Table 3. The crystal structure of alumoklyuchevskite was solved and successfully refined in the $P\overline{1}$ space group instead of the monoclinic symmetry (*I*2) reported earlier. The resulting unit-cell volume is half that previously reported. Our obtained R_1 value of 0.049 is significantly better than the previously reported value (0.131) for this mineral. New X-ray data allowed refinement of all of the atoms, including oxygens, anisotropically in contrast to data reported in Krivovichev *et al.* (2009). The calculated powder X-ray pattern in $P\overline{1}$ fits better the observed data (Table S2) than the previously obtained data in Gorskaya *et al.* (1995). The calculated pattern for the crystal structure of alumoklyuchevskite in Krivovichev *et al.* (2009) has many discrepancies with the experimental one, especially in the relatively low 2θ angle area. Atom coordinates, bond-valence sums, thermal displacement parameters and selected interatomic distances for kamchatkite and alumoklyuchevskite are provided in Supplementary Material (Tables S3–S6). Bond-valence analysis was calculated using bond-valence parameters taken from Brown & Altermatt (1985) for the Cu^{2+}–O, Na–O, S^{6+}–O, K–Cl and K–O bonds and from Allmann (1975) for Al–O bonds. Calculated values of bond-valence sums are in good agreement with the expected ones for all atoms in the structures of puninite, kamchatkite and alumoklyuchevskite.

Table 2. X-ray powder diffraction data of puninite (in Å for Co*K*α).

*I**	d_{meas}	d_{calc}	*h*	*k*	*l*
100.00	8.0576	8.0589	2	0	0
3.94	7.5961	7.6058	1	1	−1
18.88	**6.6750**	**6.6760**	**0**	**0**	**−2**
28.47	**6.4660**	**6.4704**	**2**	**0**	**−2**
5.81	4.9620	4.9322	3	1	−1
9.57	4.7451	4.7364	1	1	2
14.1	**4.3981**	**4.3944**	**2**	**0**	**2**
17.37	**4.2473**	**4.2568**	**1**	**1**	**−3**
6.96	3.9302	3.9206	3	1	−3
33.89	**3.8389**	**3.8434**	**0**	**2**	**−2**
2.87	3.5990	3.5979	2	0	−4
12.05	3.3500	3.3460	3	1	2
13.18	3.2536	3.2425	5	1	−2
4.67	3.1353	3.1405	4	2	−2
13.47	3.0609	3.0592	4	2	0
7.77	3.0373	3.0456	1	3	−1
2.4	2.9519	2.9516	1	3	1
1.48	2.9000	2.9005	1	1	4
29.15	**2.8535**	**2.857**	**2**	**2**	**−4**
2.47	2.8100	2.8126	4	2	1
14.95	**2.7240**	**2.7216**	**0**	**2**	**−4**
3.02	2.7120	2.7069	3	3	0
8.48	2.6669	2.6650	4	2	−4
8.53	2.5242	2.5223	4	2	2
5.88	2.4664	2.4661	6	2	−2
1.05	2.4003	2.4004	−7	1	2
2.11	2.3501	2.3502	0	4	0
1.14	2.3340	2.3323	6	2	0
2.46	2.2941	2.2948	−6	2	4
1.53	2.2569	2.2574	−5	3	3
1.55	2.2527	2.2562	2	4	0
1.29	2.2230	2.2253	0	0	6
2.03	2.1282	2.1284	−2	2	6
1.72	2.1220	2.1266	5	3	1
3.44	2.1071	2.1078	−4	2	6
1.24	2.0074	2.0076	6	2	2
1.64	1.9310	1.9314	3	3	4
1.92	1.8811	1.8813	−7	3	4
1.73	1.7432	1.7434	3	3	5
2.54	1.6161	1.6159	0	4	6
3.32	1.5350	1.5379	−11	1	2
1.11	1.5208	1.5212	−5	5	5
1.18	1.5065	1.5072	2	4	6

* Most intense diffraction lines in bold.

Further details of the crystal structure investigation are available from the Fachinformationszentrum Karlsruhe, D-76344 Eggenstein-Leopoldshafen, Germany, on quoting the depository number CSD–432023 (puninite), CSD–432025 (kamchatkite) and CSD–432024 (alumoklyuchevskite), along with the names of the authors and the citation of this paper.

4. Results

4.1. Cation coordination

4.1.1. Puninite

The crystal structure of puninite contains three symmetrically independent Cu sites with different coordination environments (Fig. 3a, Table 5). The Cu(1) site is coordinated by four oxygen ligands to form CuO_4 square pyramids. The Cu(2) and Cu(3) sites have a distorted square pyramidal coordination environment coordinated by five oxygen atoms each. There are two *A* sites occupied by alkali metals in the structure of puninite. The *A*(2) site is occupied exclusively by Na^+ cations, whereas the minor amount of K^+ is in *A*(1), as shown by both microprobe data and structural refinement. The *A* sites are coordinated by seven oxygen atoms each. There are three symmetrically independent sulphate sites in the puninite structure. The S^{6+} cations have typical tetrahedral coordination. The average $\langle S–O \rangle$ distances are 1.476 Å, 1.473 Å and 1.475 Å for the S(1), S(2) and S(3) sites, respectively. Generally, coordination environments of atoms in puninite are very similar to those in fedotovite, $K_2Cu_3O(SO_4)_3$ (Starova *et al.*, 1991).

The structure of puninite contains fourteen O^{2-} anions. The O(3) to O(14) atoms belong to the sulphate groups and their valence requirements are strongly influenced by the formation of S–O bonds. The O(1) and O(2) atoms (Table 6) are tetrahedrally coordinated by four Cu^{2+} cations forming short and strong O–Cu bonds. From the viewpoint of the bond-valence theory, these bonds are the strongest in the structure and thus it makes absolute sense to consider the O^{2-} anions as coordination centres for oxocentred homometallic (*i.e.* with identical metal atoms at the apices of tetrahedron) $O(1)Cu_4$ and $O(2)Cu_4$ tetrahedra. Average O–Cu bond lengths within OCu_4 tetrahedra are 1.942 Å and 1.934 Å for $O(1)Cu_4$ and $O(2)Cu_4$ tetrahedra, respectively.

4.1.2. Kamchatkite and alumoklyuchevskite

Coordination environments of atoms in kamchatkite and alumoklyuchevskite are very similar to those described earlier by Varaksina *et al.* (1990) and Krivovichev *et al.* (2009). The number of symmetrically independent oxygen atoms is reduced from seven to nine in the structure of kamchatkite according to our refinement in the *Pnma* space group. The Cu(1) and Cu(2) atoms demonstrate mixed-ligand coordination environments (Table S4) with oxygen and chlorine atoms thus forming the CuO_5Cl polyhedra also known in nabokoite (Pertlik & Zemann, 1988) and georgbokiite (Krivovichev *et al.*, 1999). The Cu(3) atoms are coordinated exclusively by oxygen thus forming Jahn-Teller distorted CuO_6 octahedra. Observed SO_4 tetrahedra (Table S4) are more regular in geometry than those in Varaksina *et al.* (1990) in accordance with the centrosymmetric space group reported in our work. One symmetrically independent K atom forms a KO_6Cl polyhedron. The O(4) atoms (Table 6) are tetrahedrally coordinated by four Cu^{2+} cations in a very symmetrical and similar manner to puninite.

The number of symmetrically independent atoms is identical in the $P\overline{1}$ (this study) and *I*2 space groups (Krivovichev *et al.*, 2009) in alumoklyuchevskite despite the different symmetry and halved volume of the unit cell. All of the Cu^{2+} cations are coordinated identically with formation of CuO_4 squares (Table S6). The *M* site has a

Table 3. Crystallographic data and structure-refinement details for puninite, kamchatkite (this study and after Varaksina *et al.*, 1990) and alumoklyuchevskite (this study and Krivovichev *et al.*, 2009).

	Puninite	Kamchatkite (this study)	Alumoklyuchevskite (this study)	Kamchatkite (Varaksina *et al.*, 1990)	Alumoklyuchevskite (Krivovichev *et al.*, 2009)
Crystal data					
Crystal system	Monoclinic	Orthorhombic	Triclinic	Orthorhombic	Monoclinic
Space group	$C2/c$	$Pnma$	$P\overline{1}$	$Pna2_1$	$I2$
Unit-cell dimensions					
a (Å)	17.3885(13)	9.755(2)	4.952(3)	9.741(5)	18.772(7)
b (Å)	9.4009(8)	7.0152(15)	11.978(6)	12.858(6)	4.967(2)
c (Å)	14.4045(11)	12.886(3)	14.626(12)	7.001(3)	18.468(7)
α (°)	90	90	87.119(9)	90	90
β (°)	112.039(2)	90	80.251(9)	90	101.66(1)
γ (°)	90	90	78.070(9)	90	90
Unit-cell volume (Å^3)	2182.6(3)	881.8(3)	836.3(9)	877(1)	1686(1)
Z	8	8	6	8	6
Calculated density (g cm^{-3})	3.298	3.565	3.001		
Absorption coeff. (mm^{-1})	6.545	8.448	5.298		
Crystal size (mm)	0.16 × 0.12 × 0.14	0.15 × 0.10 × 0.10	0.20 × 0.06 × 0.07		
Data collection					
Temperature (K)	296(2)	296(2)	296(2)		
Radiation, wavelength (Å)	Mo$K\alpha$, 0.71073	Mo$K\alpha$, 0.71073	Mo$K\alpha$, 0.71073		
F(000)	2092	908	734		
θ range (°)	2.508–27.999	2.619–35.949	1.413–21.427		
h, k, l ranges	$-22 \rightarrow 22$ $-12 \rightarrow 12$ $-18 \rightarrow 19$	$-16 \rightarrow 14$ $-11 \rightarrow 11$ $-21 \rightarrow 21$	$-5 \rightarrow 5$ $-12 \rightarrow 12$ $-15 \rightarrow 15$		
Total reflections collected	12335	14823	7154		
Unique reflections (R_{int})	2626 (0.0704)	2215 (0.0418)	1821 (0.1302)	1430	2450
Unique reflections $F > 4\sigma(F)$	1923	1895	997		
Structure refinement					
Refinement method	Full-matrix least-squares on F^2	Full-matrix least-squares on F^2	Full-matrix least-squares on F^2		
Weighting coefficients a, b	0.025700, 0.534600	0.018400, 0.443900	0.034300, 0		
Data/restraints/parameters	2626/0/194	2215/0/92	1821/12/267		
R_1 [$F > 4\sigma(F)$], wR_2 [$F > 4\sigma(F)$]	0.0349, 0.0621	0.0210, 0.0454	0.0493, 0.0945	0.055	0.131
R_2 all, wR_2 all	0.0618, 0.0706	0.0289, 0.0478	0.1015, 0.1080		
Gof on F^2	1.035	1.039	0.800		
Largest diff. peak and hole (e Å^{-3})	0.682, −0.705	0.728, −0.732	0.792, −0.780		

Table 4. Atomic coordinates and displacement parameters (Å) in puninite.

Atom	*B.V.S.*	*x*	*y*	*z*	U_{eq}	U_{11}	U_{22}	U_{33}	U_{23}	U_{13}	U_{12}
Cu(1)	1.9	0.58718(3)	0.25204(6)	0.29723(4)	0.01325(14)	0.0117(3)	0.0086(3)	0.0174(3)	0.0014(2)	0.0031(2)	0.0002(2)
Cu(2)	2.05	0.47704(3)	0.98005(6)	0.34125(4)	0.01265(14)	0.0155(3)	0.0124(3)	0.0103(3)	0.0026(2)	0.0052(2)	−0.0006(2)
Cu(3)	2.04	0.51458(3)	0.52200(6)	0.35982(4)	0.01302(14)	0.0137(3)	0.0135(3)	0.0117(3)	−0.0042(2)	0.0046(2)	−0.0010(2)
S(1)	5.99	0.66078(7)	0.96642(12)	0.36820(9)	0.0136(2)	0.0150(6)	0.0112(5)	0.0129(6)	0.0026(4)	0.0034(5)	0.0029(5)
S(2)	6.01	0.66233(7)	0.53840(12)	0.28985(9)	0.0135(2)	0.0132(6)	0.0112(5)	0.0163(6)	0.0012(5)	0.0059(5)	−0.0013(4)
S(3)	5.99	0.49178(7)	0.75065(12)	0.50868(8)	0.0116(2)	0.0162(6)	0.0095(5)	0.0098(6)	−0.0005(4)	0.0058(5)	−0.0002(4)
A(1)*	0.89	0.69695(13)	0.2537(2)	0.64380(18)	0.0404(9)	0.0185(13)	0.0399(15)	0.0585(18)	−0.0194(12)	0.0094(11)	0.0015(9)
A(2)**	1.1	0.67261(12)	0.7785(2)	0.54711(15)	0.0226(5)	0.0177(10)	0.0232(11)	0.0250(12)	0.0047(8)	0.0058(9)	0.0058(8)
O(1)	1.96	½	0.1084(4)	¼	0.0108(9)	0.013(2)	0.008(2)	0.012(2)	0.000	0.0047(19)	0.000
O(2)	2.00	½	0.3941(4)	¼	0.0118(9)	0.012(2)	0.009(2)	0.014(2)	0.000	0.0039(19)	0.000
O(3)	2.04	0.5972(2)	0.9424(3)	0.4133(3)	0.0195(8)	0.0187(18)	0.0228(19)	0.0189(19)	0.0066(14)	0.0090(15)	0.0022(14)
O(4)	2.09	0.7360(2)	0.8954(3)	0.4297(2)	0.0200(8)	0.0183(18)	0.0174(18)	0.019(2)	0.0014(14)	0.0014(15)	0.0074(14)
O(5)	1.94	0.6295(2)	0.9126(4)	0.2640(2)	0.0193(8)	0.0186(18)	0.0225(18)	0.0138(18)	−0.0011(14)	0.0026(15)	0.0080(15)
O(6)	2.07	0.67728(19)	0.1215(3)	0.3671(3)	0.0186(8)	0.0144(17)	0.0129(17)	0.025(2)	0.0044(14)	0.0029(15)	0.0015(13)
O(7)	2.11	0.67887(19)	0.3845(3)	0.3105(3)	0.0207(8)	0.0148(18)	0.0117(17)	0.034(2)	0.0049(15)	0.0067(16)	0.0011(14)
O(8)	2.03	0.73934(19)	0.6110(3)	0.3061(3)	0.0191(8)	0.0141(17)	0.0154(17)	0.027(2)	0.0011(14)	0.0061(15)	−0.0026(14)
O(9)	1.92	0.6217(2)	0.5942(4)	0.3555(2)	0.0192(8)	0.0197(18)	0.0224(19)	0.020(2)	−0.0082(15)	0.0120(15)	−0.0087(15)
O(10)	1.97	0.60651(19)	0.5561(4)	0.1824(2)	0.0190(8)	0.0136(17)	0.029(2)	0.0133(18)	0.0055(14)	0.0041(14)	−0.0037(14)
O(11)	2.09	0.44385(19)	0.8484(3)	0.4266(2)	0.0170(7)	0.0202(18)	0.0164(17)	0.0154(18)	0.0094(14)	0.0077(15)	0.0037(14)
O(12)	1.78	0.43222(19)	0.6753(3)	0.5408(2)	0.0163(7)	0.0191(18)	0.0171(18)	0.0147(18)	0.0036(13)	0.0085(15)	−0.0024(14)
O(13)	1.95	0.55330(19)	0.8297(3)	0.5915(2)	0.0159(7)	0.0193(18)	0.0165(18)	0.0120(18)	−0.0067(13)	0.0059(14)	−0.0054(14)
O(14)	2.12	0.54029(19)	0.6479(3)	0.4745(2)	0.0160(7)	0.0183(18)	0.0157(17)	0.0134(18)	−0.0085(13)	0.0050(14)	0.0013(14)

* Site population $Na_{0.930(13)}K_{0.070(13)}$.

** Site population $Na_{1.00}$.

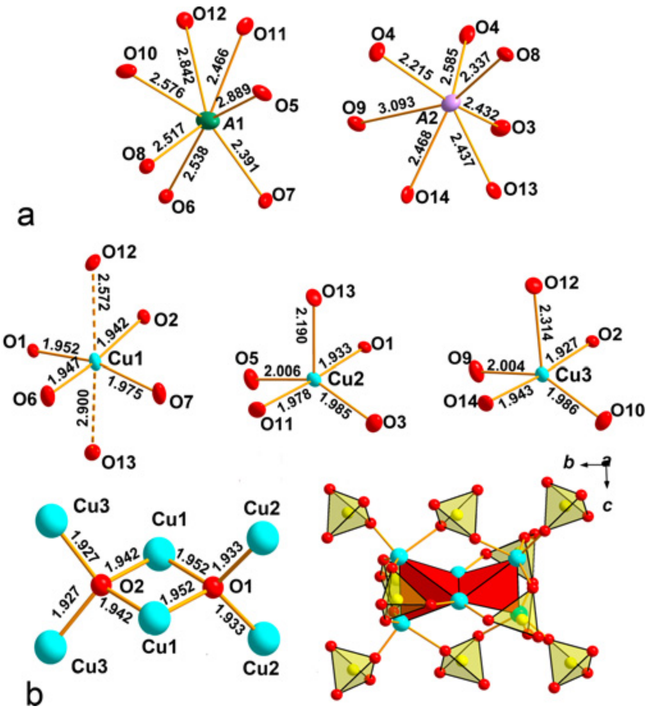

Fig. 3. Coordination of alkali *A* sites and Cu^{2+} cations in the structure of puninite (a). Ellipsoids are shown at the 50% probability level. (b) The O(1)- and O(2)-centred OCu_4 tetrahedra share a common edge thus forming $[O_2Cu_6]^{8+}$ dimers surrounded by SO_4 tetrahedra. (Online version in colour.)

Table 5. Selected interatomic distances in puninite (Å).

Cu(1)–O(2)	1.942(3)	S(3)–O(12)	1.465(3)
Cu(1)–O(6)	1.947(3)	S(3)–O(13)	1.470(3)
Cu(1)–O(1)	1.952(3)	S(3)–O(11)	1.482(3)
Cu(1)–O(7)	1.975(3)	S(3)–O(14)	1.483(3)
		⟨S–O⟩	1.475
Cu(2)–O(1)	1.933(3)		
Cu(2)–O(11)	1.978(3)	*A*(1)–O(7)	2.391(4)
Cu(2)–O(3)	1.985(3)	*A*(1)–O(11)	2.466(4)
Cu(2)–O(5)	2.006(3)	*A*(1)–O(8)	2.517(4)
Cu(2)–O(13)	2.190(3)	*A*(1)-O(6)	2.538(4)
		A(1)–O(10)	2.576(4)
Cu(3)–O(2)	1.927(3)	*A*(1)–O(12)	2.842(4)
Cu(3)–O(14)	1.943(3)	*A*(1)–O(5)	2.889(4)
Cu(3)–O(10)	1.986(3)	⟨*A*–O⟩	2.602
Cu(3)–O(9)	2.004(3)		
Cu(3)–O(12)	2.314(3)	*A*(2)–O(4)	2.215(4)
		A(2)–O(8)	2.337(4)
S(1)–O(4)	1.440(3)	*A*(2)–O(3)	2.432(4)
S(1)–O(5)	1.480(3)	*A*(2)–O(13)	2.437(4)
S(1)–O(6)	1.487(3)	*A*(2)–O(14)	2.468(4)
S(1)–O(3)	1.495(3)	*A*(2)–O(4)	2.585(4)
⟨S–O⟩	1.476	*A*(2)–O(9)	3.094(4)
		⟨*A*–O⟩	2.509
S(2)–O(8)	1.442(3)		
S(2)–O(9)	1.474(3)		
S(2)–O(7)	1.483(3)		
S(2)–O(10)	1.496(3)		
⟨S–O⟩	1.473		

mixed occupancy by Al^{3+} and Fe^{3+} cations (Table S5). Occupancy of the *M* site was first refined and later fixed in accordance with the microprobe data. The Al^{3+}/Fe^{3+} ratio in the studied alumoklyuchevskite sample is similar to that reported in Krivovichev *et al.* (2009) and Gorskaya *et al.* (1995). Coordination of the *M* site is very regular with a somewhat more symmetrical arrangement of oxygen atoms than previously reported. The SO_4 group demonstrates typical geometry and the four K sites form the following coordination polyhedra: $K(1)O_8$, $K(2)O_8$, $K(3)O_9$, $K(4)O_6$. Two symmetrically independent O(1) and O(2) are tetrahedrally coordinated, thus forming heterometallic oxocentred OCu_3M ($M = Al^{3+}$, Fe^{3+}) tetrahedra. Note that the O–*M* bond-lengths within OCu_3M tetrahedra in alumoklyuchevskite are very similar to those observed in the homometallic OCu_4 tetrahedra in puninite and kamchatkite.

4.2. Structure description

4.2.1. *Puninite*

The $O(1)Cu_4$ and $O(2)Cu_4$ tetrahedra share a common Cu (1)–Cu(1) edge (Fig. 3b) thus forming an $[O_2Cu_6]^{8+}$ dimer. Four sulphate tetrahedra are 'face-to-face' attached to the dimers, whereas the other sulphate tetrahedral groups provide their linkage in two dimensions. The resulting $\{Cu_3O(SO_4)_3\}^{2-}$ layers are parallel to the *bc* plane and the alkali atoms are in the interlayer (Fig. 4). Puninite is structurally related (Table 7) to euchlorine, $NaKCu_3O(SO_4)_3$ (Scordari & Stasi, 1990), and to fedotovite, $K_2Cu_3O(SO_4)_3$ (Starova *et al.*, 1991). There are a number of minerals and synthetic compounds structurally based on $[O_2Cu_6]^{8+}$ dimers (Kovrugin *et al.*, 2016). Such dimers can be not only homometallic but also heterometallic. In the crystal structure of another exhalative mineral from Tolbachik, prewittite, $KPb_{0.5}Cu[PbCu_5O_2]Zn(SeO_3)_2Cl_{10}$ (Shuvalov *et al.*, 2013), two adjacent heterometallic oxocentred $[OCu_3Pb]^{6+}$ tetrahedra share a common Cu . . . Pb edge to form the $[O_2Cu_5Pb]^{8+}$ dimer.

4.2.2. *Kamchatkite and alumoklyuchevskite*

The $[OCu_3]^{4+}$ chains are formed by corner-sharing oxocentred $O(4)Cu_4$ tetrahedra in the structure (Fig. 5a) of kamchatkite. The SO_4 tetrahedra surround these $[OCu_3]^{4+}$ chains and provide their linkage into a copper-oxosulphate $\{Cu_3O(SO_4)_2\}^0$ framework. KCl complexes are located in the cavities of this framework. The similar structural organization was reported for nabokoite, $Cu_7TeO_4(SO_4)_5{\cdot}KCl$ (Pertlik & Zemann, 1988), atlasovite, $Cu_6Fe^{3+}Bi^{3+}O_4(SO_4)_5{\cdot}KCl$ (Popova *et al.*, 1987) and recently for another supergene mineral, engelhauptite, $KCu_3(V_2O_7)(OH)_2Cl$ (Pekov *et al.*, 2015b), where KCl species are located in the cavities of a $\{Cu_3(V_2O_7)(OH)_2\}^0$ framework.

The chains formed by edge-sharing Cu-Cu, Cu-*M* (*M* = Al, Fe) oxocentred tetrahedra have the formula $[O_2Cu_3M^{3+}]^{5+}$ in the structure of alumoklyuchevskite

Table 6. Distances in homometallic (puninite and kamchatkite) and heterometallic (alumoklyuchevskite) oxocentred OA_4 (A = Cu, Fe^{3+}, Al^{3+}) tetrahedra.

Puninite		**Alumoklyuchevskite**	
O(1)–Cu(2)	1.933(3)×2	O(1)–Cu(2)	1.905(9)
O(1)–Cu(1)	1.952(3)×2	O(1)–Cu(1)	1.914(9)
⟨O–Cu⟩	1.942	O(1)–*M*(1)	1.936(9)
		O(1)–Cu(3)	1.937(9)
O(2)–Cu(3)	1.927(3)×2	⟨O–Cu⟩	1.923
O(2)–Cu(1)	1.942(3)×2		
⟨O–Cu⟩	1.934	O(2)–*M*(1)	1.863(10)
Kamchatkite		O(2)–Cu(2)	1.908(9)
O(4)–Cu(2)	1.9185(15)	O(2)–Cu(3)	1.937(10)
O(4)–Cu(1)	1.9211(15)	O(2)–Cu(1)	1.944(9)
O(4)–Cu(3)	1.9243(7)×2	⟨O–Cu⟩	1.913
⟨O–Cu⟩	1.922		

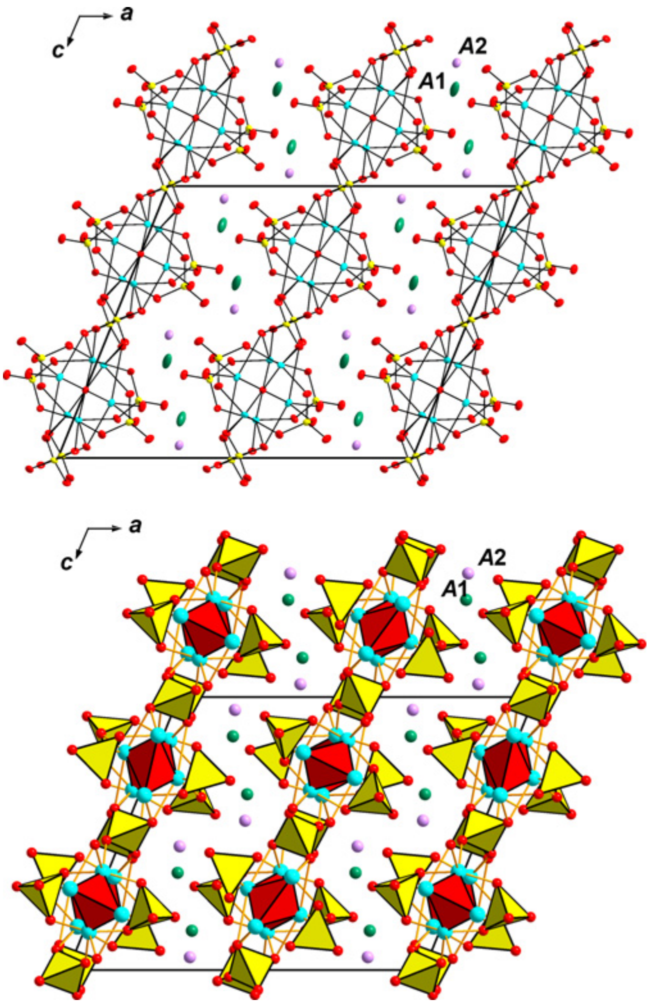

Fig. 4. General projections of the crystal structure of puninite in ball-and-stick (ellipsoids shown at 50% probability) and polyhedral representation (SO_4 = yellow, O_2Cu_6 = red) along the *b* axis. Sulphate tetrahedra and oxocentred O_2Cu_6 dimers form layers parallel to the *bc* plane. *A*(1) and *A*(2) alkali sites are located in the interlayer and highlighted. The *A*(2) site is occupied exclusively by Na, whereas minor amount of K is observed in *A*(1). (Online version in colour.)

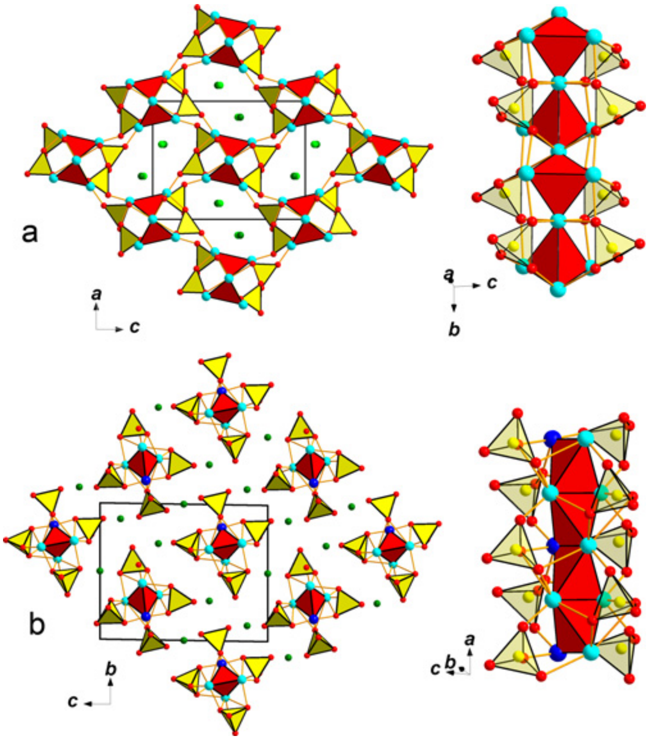

Fig. 5. General projections of the crystal structures of kamchatkite (a) and alumoklyuchevskite (b). Single $[OCu_3]^{4+}$ chains formed by corner-sharing oxocentred homometallic OCu_4 tetrahedra are surrounded by SO_4 tetrahedra in the structure of kamchatkite (above right). Single $[O_2Cu_3M^{3+}]$ (M = Al, Fe^{3+}) chains are formed by oxocentred heterometallic OCu_3M tetrahedra shared via common Cu-Cu, Cu-*M* edges in the structure of alumoklyuchevskite (below right). The K and Cl sites are shown by green and light-green balls, respectively. (Online version in colour.)

(Fig. 5b). The resulting one-dimensional copper-oxosulphate units are elongated along the *a* axis and surrounded by K atoms.

5. Discussion

The structural architecture of all the copper-oxosulphate exhalative minerals described above can be described as being organized via a "*host–guest*" principle (Fig. 6). *Guest* alkali atoms are located in between $\{Cu_3O(SO_4)_3\}^{2-}$ *host* layers in the structure of puninite (Fig. 6a). Electroneutral KCl *guest* species are located in channels of the $\{Cu_3O(SO_4)_2\}^0$ copper-oxosulphate *host* framework in the structure of kamchatkite (Fig. 6b), and K atoms surround $\{[Cu_3O_2M](SO_4)_4]\}^{3-}$ rod-like one-dimensional copper-oxosulphate units in alumoklyuchevskite (Fig. 6c). The *host–guest* character of these fumarolic minerals is possibly the result of their formation from volcanic gases. Copper-oxosulphate units of different dimensionality tend to organize in such a structure to allow the inclusion of alkali and chloride ions.

Puninite is a new member of the structural family of minerals and synthetic compounds based upon $[O_2Cu_6]^{8+}$ dimers composed from oxocentred $(OCu_4)^{6+}$ groups.

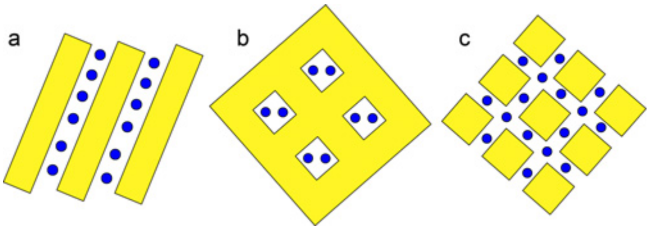

Fig. 6. Schematic representations of the crystal structures of puninite (a), kamchatkite (b) and alumoklyuchevskite (c). *Host* copper-oxosulphate structural units are symbolized by yellow and *guest* alkali (Na, K), Cl atoms by blue balls. Alkali metals are segregated in the interlayer in the structure of puninite (a). *Guest* KCl species are located in one-dimensional channels in the structure of kamchatkite (b). K atoms are in between $\{[O_2Cu_3M](SO_4)_4]\}^{3-}$ rod-like copper-oxosulphate units in alumoklyuchevskite (c). (Online version in colour.).

Table 7. Crystal-chemical data of ‘euchlorine-group’ minerals.

Mineral	Puninite	Euchlorine	Fedotovite
Formula	$NaNaCu_3O(SO_4)_3$	$KNaCu_3O(SO_4)_3$	$KKCu_3O(SO_4)_3$
Crystal system	Monoclinic		
Space group	*C*2/*c*		
Unit cell			
a, Å	17.3885(13)	18.41(5)	19.037(6)
b, Å	9.4009(8)	9.43(3)	9.479(2)
c, Å	14.4045(11)	14.21(5)	14.231(5)
β, °	112.039(2)	113.7(3)	111.04(3)
V, Å^3	2182.6(3)	2258.89(8)	2396.8(1)
Z	8	8	8
Reference	This work	Scordari & Stasi (1990)	Starova *et al.* (1991)

No direct synthetic analogues of puninite are known to date. Puninite is the first Na-dominant copper oxosulphate mineral observed on Second scoria cone. The crystal structures of puninite, euchlorine and fedotovite contain two symmetrically independent *A*(1) and *A*(2) alkali sites each (where $A = \text{Na, K}$) (Figs. 3 and 4). Thus the general crystal-chemical formula of ‘euchlorine-group’ minerals can be represented as $A(1)A(2)[Cu_3O](SO_4)_3$. In fedotovite K is dominant in both of these sites, whereas euchlorine contains one Na-dominant and one K-dominant site; in puninite, Na is dominant in both sites (Table 7). The difference in the atomic radii of K and Na manifests itself as an enlargement of the unit-cell volume for “euchlorine group” minerals from 2182.6 to 2396.8 Å^3 for puninite and fedotovite, respectively. The unit cell ‘*a*’ parameter value is very sensitive to the K/Na ratio in “euchlorine group” minerals. We have checked, using single-crystal X-ray methods, different crystals of euchlorine-like minerals from other fumaroles and assemblages (1) on the Second scoria cone of the Northern Breakthrough of the 1975 Great Fissure Eruption, and (2) on the Naboko cone of the new Tolbachik Eruption of 2012–2013. The enlargement of the ‘*a*’ parameter value is clearly correlated with increasing K content in both cases. In addition, intermediate members of the puninite (Na) – euchlorine (Na, K) – fedotovite (K) series were found. The ‘euchlorine group’ dominates in the investigated copper sulphate mineral assemblages on the scoria cones of Tolbachik (both the Great Tolbachik Fissure Eruption and the Tolbachik Fissure Eruption of 2012–2013). Taking into account the high Cs content (see Fig. 2) that is observed in these assemblages on the Second scoria cone, it is possible that a Cs-dominant member of the “euchlorine group” will be discovered in the future.

The fumaroles of Tolbachik volcano are characterized by the extremely highly oxidizing conditions, with a total absence of native sulfur and subsequent dominance of sulphate minerals. This feature is characteristic for all volcanoes of the Klyuchevskaya group. High concentrations of primary sulfuric acid in fumarolic gases were recently reported at Bezymianny volcano (Zelenski *et al.*, 2015). Such mineral-formation processes in the fumaroles of the Second scoria cone of the Northern Breakthrough of the GTFE resulted in the formation of a unique suite of primary exhalative copper-oxosulphate minerals containing 'additional' O atoms. The six most abundant trace elements observed in gases of TFE are: K (250 ppm), Na (220 ppm), Si (74 ppm), Br (48 ppm), Cu (21 ppm) and Fe (12 ppm) (Zelenski *et al.*, 2014); they explain the wide distribution of alkali copper oxosulfates in these fumarolic mineral assemblages. Similar processes, but at much smaller scale, have been detected in other volcanoes such as Vesuvius (Italy). Note that most sulphates at these localities are secondary and that exhalative mineral assemblages are dominated by sulphides (S^{2-}) and sulphosalts in accordance with the two following reactions: (1) $H_2S + 1/2O_2 = S + H_2O$ and (2) $2H_2S + SO_2 = 2S + 2H_2O$ (Giggenbach, 1987). However, this is not the case for Tolbachik. Thermodynamic calculations are needed to explain the fractionation of elements and subsequent formation of unique mineral assemblages observed in fumaroles of scoria cones of Tolbachik volcano. We are in the progress to obtain ‘pure’ synthetic analogues of copper oxosulphate minerals, unavailable to date, for this purpose by chemical vapour transport (CVT) reactions. Recent studies revealed this method to be very efficient to emulate exhalative chemistry in laboratory conditions (Kovrugin *et al.*, 2015).

Acknowledgements: This work was financially supported by the Russian Science Foundation through the grant 16-17-10085. Technical support by the SPbSU X-ray Diffraction Resource Centre and Geomodel Resource Center are gratefully acknowledged.

References

Allmann, R. (1975): Beziehungen zwischen Bindungslängen und Bindungsstärken in Oxidstrukturen. *Monatsh. Chem.*, **106**, 779–793.

Alpers, C.N., Jambor, J.L., Nordstrom, D.K. (2000): Sulfate minerals: crystallography, geochemistry, and environmental significance. *Rev. Mineral. Geochem.*, **40**, 1–602.

Brown, I.D. & Altermatt, D. (1985): Bond-valence parameters obtained from a systematic analysis of the Inorganic Crystal Structure Database. *Acta Crystallogr.*, **B41**, 244–247.

Bykova, E.Y., Berlepsch, P., Kartashov, P.M., Armbruster, Th. (1998): Vergasovaite $Cu_3O[(Mo,S)O_4][SO_4]$, a new copper oxymolybdate sulphate from Kamchatka. *Schweiz. Mineral. Petrogr. Mitt.*, **78**, 479–488.

Effenberger, H. (1985): $Cu_2O(SO_4)$, dolerophanite: refinement of the crystal structure with a comparison of $OCu(II)_4$ tetrahedra in inorganic compounds. *Monatsh. Chem.*, **116**, 927–931.

Fedotov, S.A. & Markhinin, Y.K., eds. (1983): The Great Tolbachik Fissure Eruption. Cambridge Univ. Press, New York.

Filatov, S.K. & Vergasova, L.P. (1989): On descrediting of caratiite and priority of piypite. *Zap. Vsesoyuzn. Mineral. O-va*, **118**, 88–90.

Filatov, S.K., Semenova, T.F., Vergasova, L.P. (1992): Types of polymerization of tetrahedra $[OCu_4]^{6+}$ in compounds with additional atoms of oxygen. *Dokl. Akad. Nauk SSSR*, **322**, 536–539.

Giggenbach, W.F. (1987): Redox processes governing the chemistry of fumarolic gas discharges from White Island, New Zealand. *Appl. Geochem.*, **2**, 143–161.

Gorskaya, M.G., Vergasova, L.P., Filatov, S.K., Rolich, D.V., Ananiev, V.V. (1995): Alumoklyuchevskite, $K_3Cu_3AlO_2(SO_4)_4$, a new oxosulphate of K, Cu and Al from volcanic exhalations, Kamchatka, Russia. *Zap. Vseross. Mineral. O-va*, **124**, 95–100.

Kovrugin, V.M., Siidra, O.I., Colmont, M., Mentré, O., Krivovichev, S.V. (2015): Emulating exhalative chemistry: synthesis and structural characterization of ilinskite, $Na[Cu_5O_2](SeO_3)_2Cl_3$, and its K-analogue. *Mineral. Petrol.*, **109**, 421–430.

Kovrugin, V.M., Colmont, M., Mentré, O., Siidra, O.I., Krivovichev, S.V. (2016): Dimers of oxocentred $[OCu_4]^{6+}$ tetrahedra in two novel copper selenite chlorides, $K[Cu_3O](SeO_3)_2Cl$ and $Na_2[Cu_7O_2](SeO_3)_4Cl_4$, and related minerals and inorganic compounds. *Mineral. Mag.*, **80**, 227–238.

Krivovichev, S.V., Shuvalov, R.R., Semenova, T.F., Filatov, S.K. (1999): Crystal chemistry of inorganic compounds based on chains of oxocentered tetrahedra. III. Crystal structure of georgbokiite, $Cu_5O_2(SeO_3)_2Cl_2$. *Z. Kristallogr.*, **214**, 135–138.

Krivovichev, S.V., Filatov, S.K., Cherepansky, P.N. (2009): The crystal structure of alumoklyuchevskite, $K_3Cu_3AlO_2(SO_4)_4$. *Geol. Ore Deposits*, **51**, 656–662.

Krivovichev, S.V., Mentré, O., Siidra, O.I., Colmont, M., Filatov, S. K. (2013): Anion-centered tetrahedra in inorganic compounds. *Chem. Rev.*, **113**, 6459–6535.

Mandarino, J.A. (1981): The Gladstone-Dale relationship. Part IV. The compatibility concept and its application. *Can. Mineral.*, **14**, 498–502.

Marsh, R.E. (1995): Some thoughts on choosing the correct space group. *Acta Crystallogr.*, **B51**, 897–907.

Meniaylov, I.A., Nikitina, L.P., Shapar', V.N. (1980): Geochemical Features of Exhalations of the Great Tolbachik Fissure Eruption. Nauka Publishing, Moscow, 235 p. (in Russian).

Pekov, I.V., Zubkova, N.V., Yapaskurt, V.O., Belakovskiy, D.I., Chukanov, N.V., Lykova, I.S., Savelyev, D.P., Sidorov, E.G., Pushcharovsky, D.Yu. (2014): Wulffite, $K_3NaCu_4O_2(SO_4)_4$, and parawulffite, $K_5Na_3Cu_8O_4(SO_4)_8$, two new minerals from fumarole sublimates of the Tolbachik Volcano, Kamchatka, Russia. *Can. Mineral.*, **52**, 699–716.

Pekov I.V., Zubkova N.V., Belakovskiy D.I., Lykova I.S., Yapaskurt V.O., Vigasina M.F., Sidorov E.G., Pushcharovsky D.Yu. (2015a): Sanguite, $KCuCl_3$, a new mineral from the Tolbachik volcano, Kamchatka, Russia. *Can. Mineral.*, **53**, 633–641.

Pekov, I.V., Siidra, O.I., Chukanov, N.V., Yapaskurt, V.O., Britvin, S.N., Krivovichev, S.V., Schüller, W., Ternes, B. (2015b): Engelhauptite, $KCu_3(V_2O_7)(OH)_2Cl$, a new mineral species from Eifel, Germany. *Mineral. Petrol.*, **109**, 705–711.

Pekov, I.V., Zubkova, N.V., Agakhanov, A.A., Yapaskurt, V.O., Belakovskiy, D.I., Vigasina, M.F., Sidorov, E.G., Pushcharovsky, D.Y. (2015c): Cryptochalcite, IMA 2014-106. CNMNC Newsletter No. 25. *Mineral. Mag.*, **79**, 530.

Pertlik, F. & Zemann, J. (1988): The crystal structure of nabokoite, $Cu_7TeO_4(SO_4)_5{\cdot}KCl$: the first example of a $Te(IV)O_4$ pyramid with exactly tetragonal symmetry. *Mineral. Petrol.*, **38**, 291–298.

Popova, V.I., Popov, V.A., Rudashevskii, N.S., Glavatskikh, S.F., Polyakov, V.O., Bushmakin, A.F. (1987): Nabokoite, $Cu_7TeO_4(SO_4)_5{\cdot}KCl$ and atlasovite, $Cu_6Fe^{3+}Bi^{3+}O_4(SO_4)_5{\cdot}KCl$: new minerals of volcanic exhalations. *Zap. Vsesoyuzn. Mineral. O-va*, **116**, 358–367.

Scordari, F. & Stasi, F. (1990): The crystal structure of euchlorine, $NaKCu_3O(SO_4)_3$. *N. Jb. Miner. Abh.*, **161**, 241–253.

Sheldrick, G.M. (2015): New features added to the refinement program SHELXL since 2008 are described and explained. *Acta Crystallogr.*, **C71**, 3–8.

Shuvalov, R.R., Vergasova, L.P., Semenova, T.F., Filatov, S.K., Krivovichev, S.V., Siidra, O.I., Rudashevsky, N.S. (2013): Prewittite, $KPb_{1.5}Cu_6Zn(SeO_3)_2O_2Cl_{10}$, a new mineral from Tolbachik fumaroles, Kamchatka peninsula, Russia: Description and crystal structure. *Am. Mineral.*, **98**, 463–469.

Starova, G.L., Filatov, S.K., Fundamenskii, V.S., Vergasova, L.P. (1991): The crystal structure of fedotovite, $K_2Cu_3O(SO_4)_3$. *Mineral. Mag.*, **55**, 613–616.

Varaksina, T.V., Fundamensky, V.S., Filatov, S.K., Vergasova, L.P. (1990): The crystal structure of kamchatkite, a new naturally occurring oxychloride sulphate of potassium and copper. *Mineral. Mag.*, **54**, 613–616.

Vergasova, L.P. & Filatov, S.K. (2012): New mineral species in products of fumarole activity of the Great Tolbachik Fissure Eruption. *J. Volcanol. Seismol.*, **6**, 281–289.

Vergasova, L.P., Filatov, S.K., Serafimova, E.K., Starova, G.L. (1988a): Fedotovite, $K_2Cu_3O(SO_4)_3$, a new mineral of volcanic sublimates. *Dokl. Akad. Nauk SSSR*, **299**, 961–964.

Vergasova, L.P., Filatov, S.K., Serafimova, E.K., Varaksina, T.V. (1988b): Kamchatkite, $KCu_3OCl(SO_4)_2$, a new mineral of volcanic sublimates. *Zap. Vsesoyuzn. Mineral. O-va*, **117**, 459–461.

Vergasova, L.P., Filatov, S.K., Gorskaya, M.G., Ananiev, V.V., Sharov, A.S. (1989): Klyuchevskite, $K_3Cu_3Fe^{3+}O_2(SO_4)_4$, a new mineral of volcanic sublimates. *Zap. Vsesoyuzn. Mineral. O-va*, **118**, 70–73.

Volynets, A., Melnikov, D., Yakushev, A. (2013): First data on composition of the volcanic rocks of the IVS 50th anniversary Fissure Tolbachik Eruption. *Doklady Earth Sci.*, **452**, 953–957.

Zelenski, M., Malik, N., Taran, Y. (2014): Emissions of trace elements during the 2012–2013 effusive eruption of Tolbachik volcano, Kamchatka: enrichment factors, partition coefficients and aerosol contribution. *J. Volcanol. Geotherm. Res.*, **285**, 136–149.

Zelenski, M., Taran, Y., Galle, B. (2015): High emission rate of sulfuric acid from Bezymianny volcano, Kamchatka. *Geophys. Res. Lett.*, **42**, 7005–7013.

Received 17 October 2016
Modified version received 20 November 2016
Accepted 23 November 2016

Eur. J. Mineral.
2017, **29**, 1089

Erratum

Copper oxosulphates from fumaroles of Tolbachik volcano: puninite, $Na_2Cu_3O(SO_4)_3$ – a new mineral species and structure refinements of kamchatkite and alumoklyuchevskite by Oleg I. Siidra*, Evgenii V. Nazarchuk, Anatoly N. Zaitsev, Evgeniya A. Lukina, Evgeniya Y. Avdontseva, Lidiya P. Vergasova, Natalia S. Vlasenko, Stanislav K. Filatov, Rick Turner, Gennady A. Karpov (2017, vol. **29**, p. 499–510, DOI: 10.1127/ejm/2017/0029-2619)

*Corresponding author, e-mail: siidra@mail.ru

The optical data for puninite were erroneously reported in the abstract as $\alpha = 1.587(2)$, $\beta = 1.611(2)$, $\gamma = 1.649(2)$, $2V_{calc} = 60°$. The correct values are $\alpha = 1.562(2)$, $\beta = 1.591(2)$, $\gamma = 1.634(2)$ (589 nm), $2V_{calc} = 80.7°$, as indicated in the main text on page 500 (part 3.1, Physical and optical properties of puninite). These errors do not affect the essentials of the study, but the authors and editors offer apologies for any inconvenience.

DOI: 10.1127/ejm/2017/0029-2705

0935-1221/17/0029-2705 $ 0.45